Hybrid Superelliptic Horn

J.A.G. Malherbe
Department of Electrical, Electronic and Computer Engineering
University of Pretoria
Pretoria 0002, South Africa
jagm@up.ac.za

ABSTRACT - *The waveguide horn with elliptic flare has been shown to exhibit superior radiation and impedance properties. In this paper a horn is described that flares with a hybrid superelliptical profile. The radiation patterns in the principal planes are identical up to the -10 dB points.*

Key words: Waveguide horn, superelliptic profile.

1 INTRODUCTION

Conventional pyramidal waveguide horns are popular structures and widely applied as primary radiators, feeds for reflector antenna systems, etc. By modifying the linear flare of the pyramidal horn to an elliptic flare, it was shown in [1] that it is possible to dramatically improve the matching of the horn, as well as to eliminate the sidelobes. While the radiation patterns of the elliptical horn did not vary as much as those of linear pyramidal horns, the radiation patterns in the principal planes retained the same shape, but the E-plane pattern was generally 10° wider than the H-plane pattern at the -10 dB beamwidth. This is of course due to the fact that the H-plane pattern has an inherent null due to the electric field distribution. Clearly, the radiation patterns are affected by the horn flare [1] – [4] where in [4] it was shown that performance as a function of frequency could also be controlled. The return loss is also influenced to a large extent by the shape of the source region (the "throat") [1], [2].

In order to be able to separately adjust the flare of the horn in different regions such as at the throat and the aperture region, a different type of flare was investigated and employed. The general family of superellipses, of which the standard ellipse is one, do exhibit such properties. In this paper it is shown that by judicious choice of the superellipse parameters, a waveguide horn can be designed that has almost identical radiation patterns in the principal planes up to the -10 dB points.

2 SUPERELLIPTIC FUNCTIONS

The general parametric form of an ellipse is given by

$$\left.\begin{aligned} u(\theta) &= a\left|\cos\theta\right|^{2/m} \\ v(\theta) &= b\left|\sin\theta\right|^{2/n} \end{aligned}\right\} m,n > 0 \tag{1}$$

For *m,n* < 2, the resultant curve is termed a hypoellipse, and for *m,n* > 2, a hyperellipse results. Fig. 1 compares one quarter of respectively a standard ellipse (*m* = *n* = 2), a hypoellipse with *m* = *n* = 1 and a hyperellipse with *m* = *n* = 4. Note that all the curves are tangential to the intersections with the major axes, i.e. the slope is zero at *u* = 0, and vertical at *u* = *a*. Of course, the values of *m* and *n* need not be the same, and this makes it possible to introduce different shapes, for instance, to the throat of the horn, than for the aperture region.

A heuristic evaluation of the effects of the shape of the horn flare on the radiation patterns showed that it was necessary to maintain the horn width at the throat, but to flare less rapidly towards the aperture. The latter can be achieved by employing a hyperellipse, but this drastically reduces the throat flare, as can be seen from Fig. 1. Conversely, a hypoellipse flares too rapidly. A combination of the properties of these elliptical forms can be obtained by correct choice of m and n. Also shown in Fig. 1 is a superellipse for which $m = 4$ and $n = 4/3$, i.e. a mixture of hypo- and hyperellipse, which has been termed a hybrid (super)ellipse.
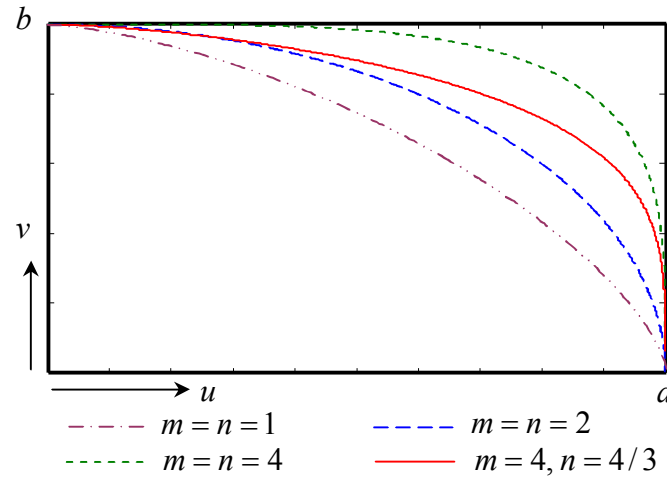

Fig. 1. Comparison of a standard ellipse with a hypo-
hyper- and hybrid elliptical form

3 HYBRID ELLIPTIC HORN

Referring to Fig. 2, if the waveguide has dimensions of $2y_0$ x $2z_0$, and the aperture measures $2y_a$ x $2z_a$, with a total horn length of l, the metallic edges that make up the horn are described by the parametric expressions

$$\left. \begin{array}{c} y(\theta) = y_a - (y_a - y_0)\cos^{0.5}\theta \\ z(\theta) = z_a - (z_a - z_0)\cos^{0.5}\theta \\ x(\theta) = l\sin^{1.5}\theta \\ 0 \le \theta \le \pi/2 \end{array} \right\} \qquad (2)$$

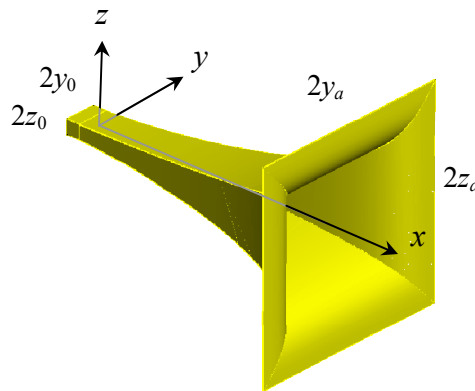where $m = 4$ across the width (y) and height (z) and $n = 4/3$ along the length (x) of the horn.

Fig. 2. Isometric horn view

A vertical cross section (*x-z*) of the horn is shown in Fig. 3; also shown is the shape of a standard ellipse, with parametric equations

$$z(\theta) = z_a - (z_a - z_0)\cos\theta$$
$$x(\theta) = l\sin\theta$$
$$0 \leq \theta \leq \pi/2$$

(3)

Note that the hybrid elliptic horn opens more rapidly at the throat, but flares more slowly at the aperture.
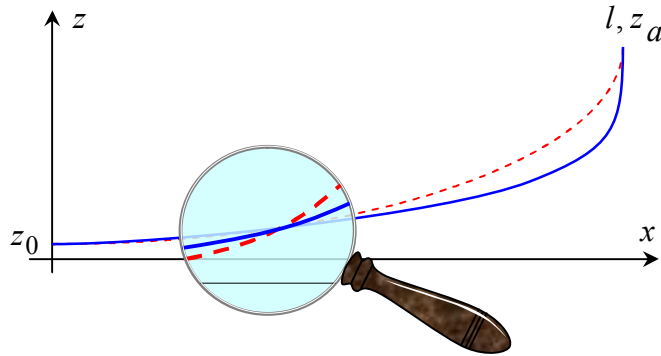

Fig. 3. Comparison of the hybrid elliptic horn
profile ——— to that of a standard elliptic profile - - - - .

4 HORN PERFORMANCE

A hybrid elliptic horn for X-band with dimensions $2y_0 = 22.86 \times 2z_0 = 10.16$ mm, aperture $2y_a = 2z_a = 150$ mm, and length $l = 200$ mm was analyzed numerically by means of FEKO [5], and then constructed from 0.7 mm brass plate and fitted with a standard X-band waveguide flange.

The gain, input reflection coefficient, and principal plane radiation patterns were calculated and measured for frequencies between 8 and 12 GHz. Fig. 4 shows the calculated and measured values for gain and reflection coefficient. The gain varies between 15.5 and 18.0 dB. The calculated return loss is lower than -45 dB, while the measured values lie below -32 dB.
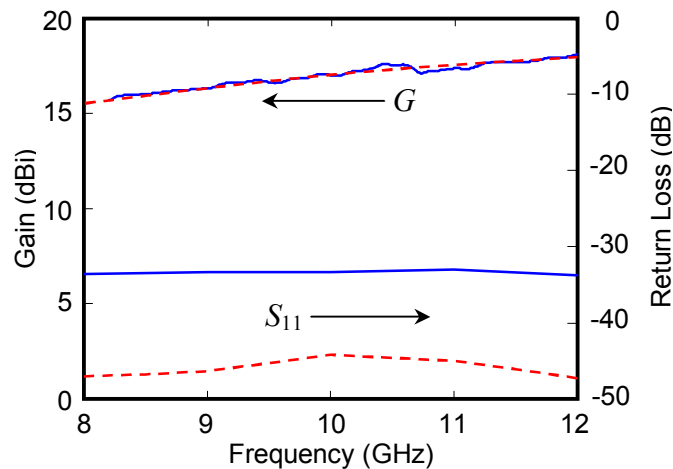

Fig. 4. Calculated - - - - - and measured ——— values
of Gain and Return Loss

The principal plane radiation patterns are shown in Fig. 5 for both calculated and measured values. For clarity, only the curves at 8 and 12 GHz are shown; the curves for 9, 10 and 11GHz lie evenly spaced in between.
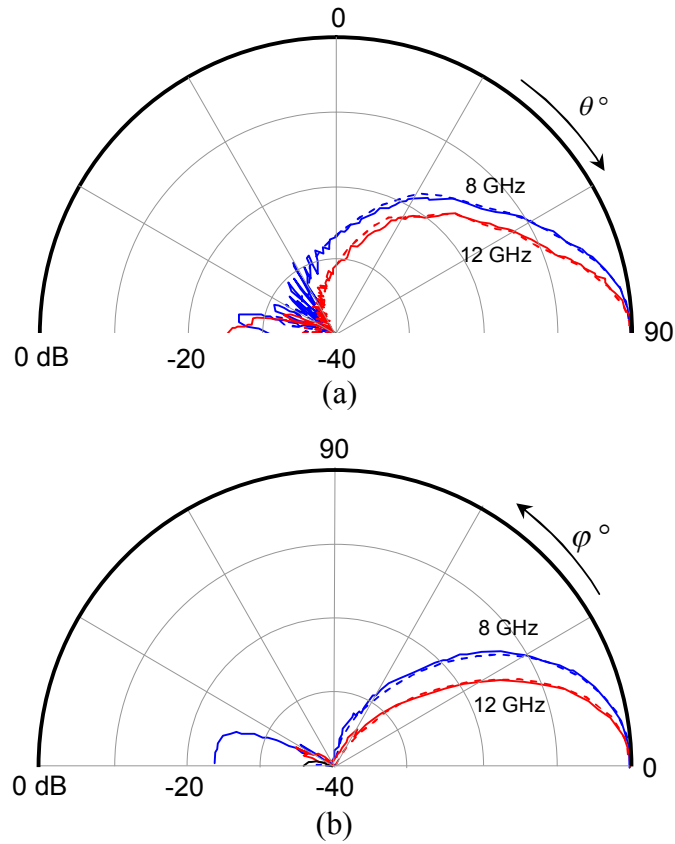

(a)

(b)

Fig. 5. Comparison of calculated - - - - - - and measured ———— radiation patterns at 8 and 12 GHz. (a) E-Plane, and (b) H-Plane.

In Fig. 6 the E- and H-plane radiation patterns are superimposed; the angle α is measured from the antenna boresight. Once again only the 8 and 12 GHz curves are shown for clarity.
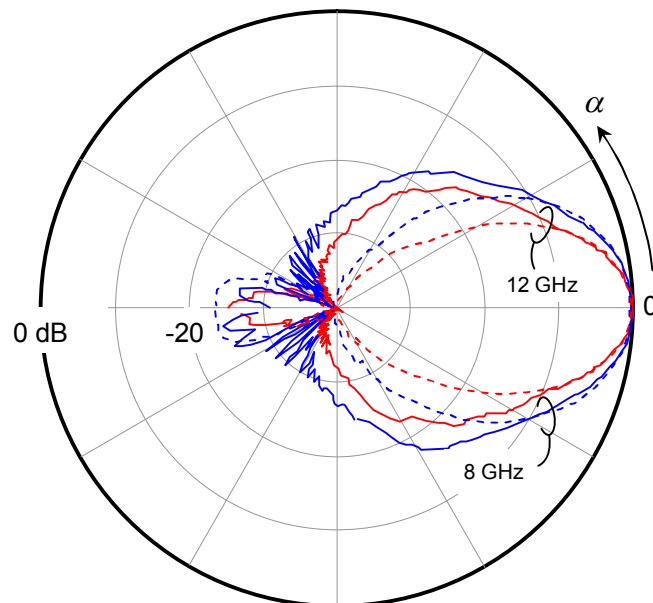

Fig. 6. Superimposed measured radiation patterns for E ———— and H - - - - - - planes at 8 and 12 GHz.

Fig. 7 shows the main beam (E_θ) radiation patterns on a spherical surface in the far field, described by the conical angles α and β as defined in the figure. It is seen that, up to the -10 dB points, the radiation patterns vary by less than ±0.5 dB from the circular. At 8 GHz, the beam is approximately 60° wide for all values of α, while the corresponding beamwidth at 12 GHz is approximately 40°.
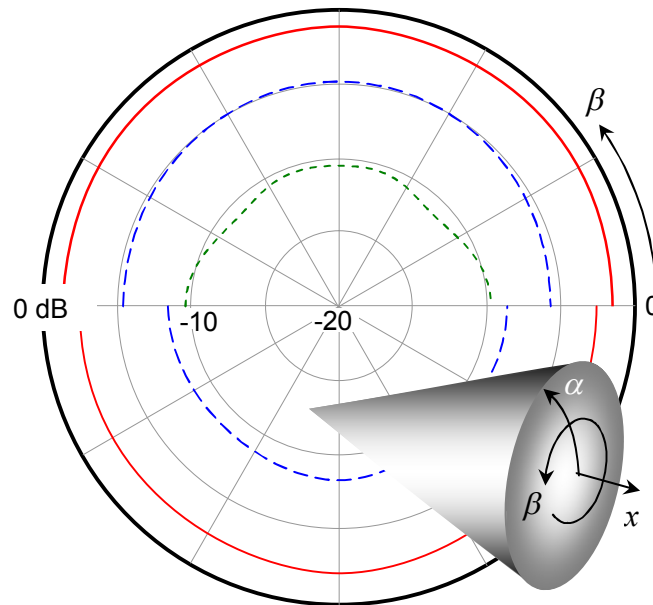

Fig. 7. Conical radiation patterns. Upper hemisphere:
8 GHz, $0 \le \beta \le 360°$, $\alpha = 10°$ ——— , 20° – – – , 30° ———;
Lower hemisphere: 12 GHz, $0 \le \beta \le 360°$ ($\alpha = 10°$ and 20°).

Fig. 8 shows 3D radiation patterns at 8 GHz. The co-polarized field, E_θ, is shown in Fig. 8(a); the main beam is symmetrical about the x–axis to -10 dB as shown in Fig. 7. The cross-polarized field, E_φ, is shown in Fig. 8(b).
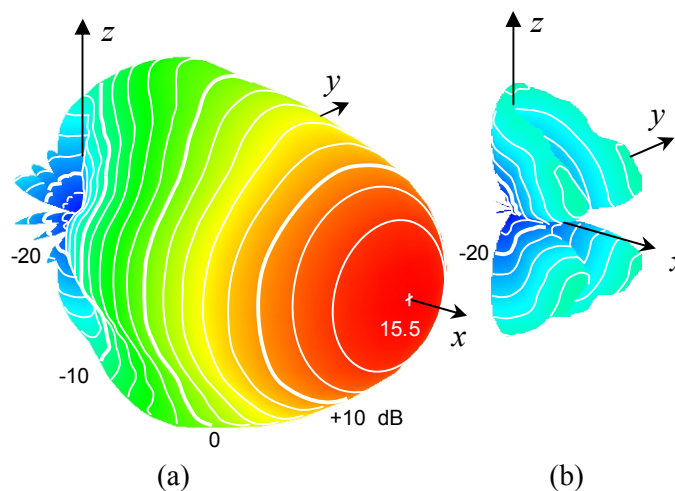

(a)   (b)

Fig. 8. 3D radiation patterns showing
(a), E_θ, and (b), E_φ in dB on the same scale, at 8 GHz.

The cross-polarization level at $\{\theta = 60, 90°; 0 \le \varphi \le 30°\}$ is shown in Fig. 9 for 8 and 12 GHz. It remains below -50 dB on the main axes, and below -10 dB within the beam solid angle.
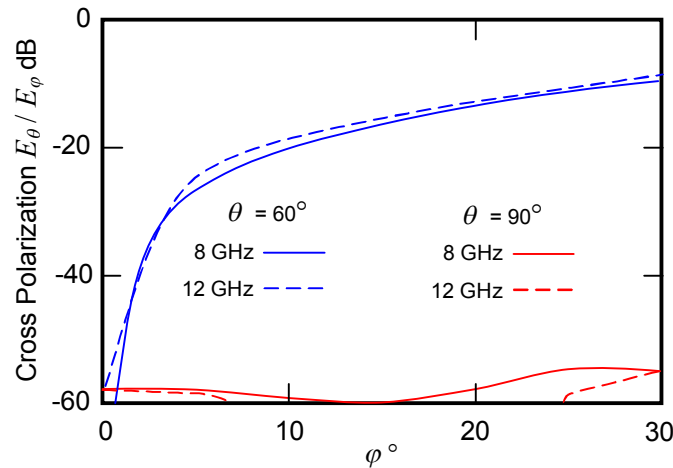

Fig. 9. Ratio of co-polarized (E_θ) to cross-polarized (E_φ) field at 8 and 12 GHz.

5 CONCLUSION

It has been shown that by choosing the surfaces of a waveguide horn to be described by a pair of hybrid ellipses, excellent performance can be obtained. The measured return loss is some 10 dB higher than the calculated value; however, the measured level corresponds to the lowest return loss that can be measured with the waveguide measurement system. The agreement between calculated and measured gain values is excellent.

The radiation pattern remains symmetrical about the boresight up to a beamwidth of -10 dB at all frequencies, and the correlation between calculated and measured patterns is once again excellent.

REFERENCES

[1] J.A.G. Malherbe and Y. Katcodia, "An Elliptically Flared Waveguide Horn**",** *Microwave Opt Tehcnol Lett*, Vol. 52, no. 9, pp. 2118-2120, Sept. 2010.

[2] H. Henke, "Influence of the Wall Geometry on Reflection and Transmission in an E-Plane Sectoral Horn", *IEEE Trans. Antennas Propagat.*, Vo. 25, No. 4, pp. 556-560, Jul. 1977.

[3] W.D. Burnside and C.W. Chuang, "An Aperture-Matched Horn Design", *IEEE Trans. Antennas Propagat.*, Vol. 30, No. 4, pp. 790-796, July 1982.

[4] J.A.G. Malherbe, "Frequency-Independent Performance of Elliptic Profile TEM Horns", *Microwave Optical Tech. Lett*, Vol. 51, No. 3, pp. 607-612, March 2009.

[5] FEKO™, EM Software & Systems-S.A. (Pty) Ltd. http://www.feko.info/index.html.